Biomedical Physics & Engineering
Express

Endorsed by IPEM
Institute of Physics and
Engineering in Medicine

PAPER

The role of beat-by-beat cardiac features in machine learning classification of ischemic heart disease (IHD) in magnetocardiogram (MCG)

To cite this article: S Senthilnathan *et al* 2024 *Biomed. Phys. Eng. Express* **10** 045007

IOP Publishing Biomed. Phys. Eng. Express 10 (2024) 045007 https://doi.org/10.1088/2057-1976/ad40b1

Biomedical Physics & Engineering Express

CrossMark

RECEIVED
7 August 2023

REVISED
31 March 2024

ACCEPTED FOR PUBLICATION
19 April 2024

PUBLISHED
7 May 2024

PAPER

The role of beat-by-beat cardiac features in machine learning classification of ischemic heart disease (IHD) in magnetocardiogram (MCG)

S Senthilnathan[1,*], **S Shenbaga Devi**[2], **M Sasikala**[2], **Santhosh Satheesh**[3] **and Raja J Selvaraj**[3]

[1] SQUIDs Applications Section, SQUID and Detector Technology Division, Materials Science Group, Indira Gandhi Centre for Atomic Research, Kalpakkam-603 102, Tamil Nadu, India
[2] Centre for Medical Electronics, Department of Electronics and Communication Engineering, Anna University, Chennai-600 025, Tamil Nadu, India
[3] Department of Cardiology, Jawaharlal Institute of Postgraduate Medical Education and Research, Dhanvantri Nagar, Pondicherry-605 006, Puducherry, India
[*] Author to whom any correspondence should be addressed.

E-mail: sengo@igcar.gov.in **and** sengottuvelnvs@gmail.com

Keywords: ischemic heart disease, myocardial infarction, machine learning classifiers, magnetocardiography, beat-by-beat cardiac features

Supplementary material for this article is available online

Abstract

Cardiac electrical changes associated with ischemic heart disease (IHD) are subtle and could be detected even in rest condition in magnetocardiography (MCG) which measures weak cardiac magnetic fields. Cardiac features that are derived from MCG recorded from multiple locations on the chest of subjects and some conventional time domain indices are widely used in Machine learning (ML) classifiers to objectively distinguish IHD and control subjects. Most of the earlier studies have employed features that are derived from signal-averaged cardiac beats and have ignored inter-beat information. The present study demonstrates the utility of beat-by-beat features to be useful in classifying IHD subjects (n = 23) and healthy controls (n = 75) in 37-channel MCG data taken under rest condition of subjects. The study reveals the importance of three features (out of eight measured features) namely, the field map angle (FMA) computed from magnetic field map, beat-by-beat variations of alpha angle in the ST-T region and T wave magnitude variations in yielding a better classification accuracy (92.7 %) against that achieved by conventional features (81 %). Further, beat-by-beat features are also found to augment the accuracy in classifying myocardial infarction (MI) Versus control subjects in two public ECG databases (92 % from 88 % and 94 % from 77 %). These demonstrations summarily suggest the importance of beat-by-beat features in clinical diagnosis of ischemia.

1. Introduction

Cardiovascular diseases are one of the major causes of death in developing countries with an age-standardized global average of 235 per one Lakh population and of which, mortality attributed to ischemic heart disease (IHD) alone is 115 per one Lakh population [1]. The global prevalence rate of IHD is currently estimated to be 1655 per one Lakh population and is expected to exceed 1845 per one Lakh population by 2030 [2]. These alarmingly increasing numbers have raised global concerns and since an unattended IHD might cause myocardial infarction (MI), an early diagnosis at the stage of ischemia is considered quintessential. While the electrical manifestations pertaining to MI are straight forward to be detected in ECG, signal variations at an early stage in IHD are subtle in nature and could only be detected under stress conditions [3]. In this context, noninvasive and noncontact technique of measuring weak magnetic fields generated by cardiac electrical activity, namely, the magnetocardiography (MCG) is sensitive in measuring ischemic changes under rest itself [4–8]. Recent studies justify the choice of MCG in emergency wards to reduce the triaging time to be helpful in the clinical management of IHD [9].

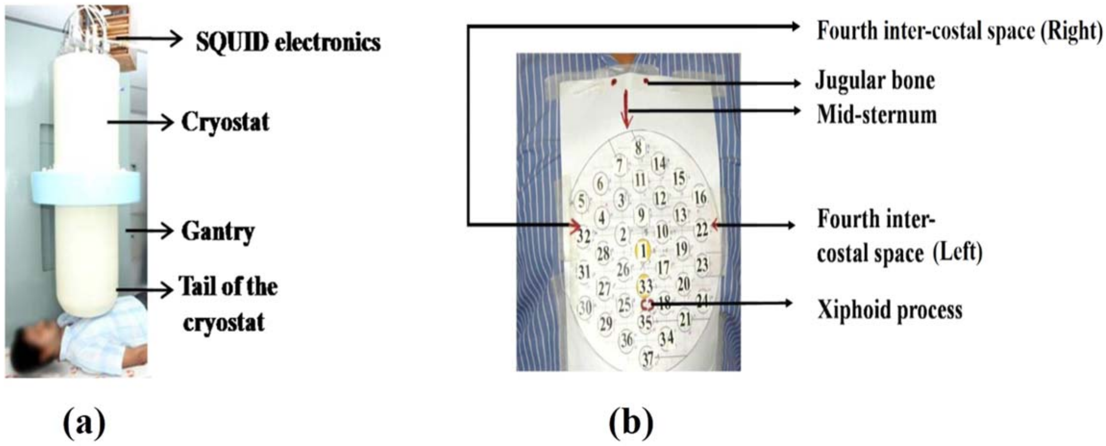

Figure 1. Photographs of the MCG experimental setup used for data collection and the measurement grid (a) 37-channel SQUID-based MCG set up consisting of liquid Helium cryostat mounted on a nonmagnetic gantry with a subject positioned for measurement (b) Photograph of the hexagonal measurement grid pasted on the chest of a subject marked with sensor positions.

Various studies have reported qualitative differences in magnetic field maps generated from the spatial-temporal distribution patterns of MCG of subjects with IHD against healthy controls [5, 10]. A more objective way to distinguish subjects with IHD is achieved by machine learning (ML) classifiers using time domain, frequency domain, spatial distribution measures and information theory parameters quantified from the ST-T region of the MCG cardiac beats as feature sets [11–19]. Most of these MCG studies have reported deriving cardiac features from representative signal-averaged cardiac beat by averaging several cardiac cycles of the time series to achieve an improvement in the signal-to-noise ratio (SNR) of features. However, the averaging process is known to destroy inter-beat cardiac variations [20]. The existence of beat-by-beat variations in ST-T region (the signal region of interest to measure ischemic variations) of the cardiac cycle is reported in MI subjects [21, 22]. Considering the proven sensitivity of MCG in detecting IHD (which precedes MI), it is persuading to explore the significance of inter-beat dynamics of MCG time series in ML classification of IHD in addition to that of the conventional features. Further, this study details the importance of inter-beat features in classifying MI and healthy controls by exclusively demonstrating their roles on ECG time series taken from two public databases.

The paper is organized as follows: a brief introduction to the experimental set up employed in this work for the collection of MCG data, MCG signal processing and measurement of features for ML classification are discussed in section 2. Results on the utility of standard and the beat-by-beat features in the ML classification of IHD in MCG and their utility in MI detection demonstrated on two ECG databases are detailed in section 3. Section 4 discusses the comparison of the results with recent reports in the literature. Finally, the conclusions are presented in section 5.

2. Materials & methods

2.1. Experimental setup and data collection

Figure 1 shows the photographs of the MCG system and measurement grid used in this work for data collection. Figure 1(a) shows the MCG system which consists of thirty-seven superconducting quantum interference device (SQUID) sensors populated in an insert as a hexagonal array positioned inside a cryostat filled with liquid Helium [23, 24]. The setup is kept inside a moderate magnetically shielded room (MSR) to attenuate low and high-frequency electromagnetic ambient noise. The coupling of the input flux to the SQUID sensors is achieved by superconducting first-order axial gradiometers [24]. The setup has an average noise floor of 22 femto Tesla/$\sqrt{}$Hz (of 37 channels) at a bandwidth of 0–300 Hz. The sensor outputs of all the measurement channels are digitized at a sampling rate of 1000 Hz. Figure 1(b) shows the paper grid containing the actual positions of sensors in the array marked with anatomical landmarks which define the boundary of the heart. Each measurement session lasts for 5 min with subjects lying relaxed in a non-magnetic bed. MCG signals are simultaneously digitized, and stored for offline analysis.

2.2. Subject groups

MCG data of two groups of subjects are used in this analysis, a healthy group ($n = 75$) and IHD group ($n = 23$). The healthy group consists of young volunteers (57 Male, 18 female of age group 30 ± 7 years). The volunteers of the control group do not have history of any cardiovascular disease, neither reported of any complaint associated with cardiac health. Further, no significant abnormal electrical changes are observed in their ECGs as interpreted by a cardiologist and are hence designated as 'healthy controls.' The subjects of IHD group (14 Male, 9 female of age group 45 ± 25 years) are selected based on a clinical examination. Coronary blocks are suspected on these subjects based on horizontal or down-sloping ST segment ($> 100\ \mu$V) in treadmill ECG test following the clinical criteria for diagnosing IHD [3]. MCG is recorded from all these subjects before subjecting them for coronary angiogram. MCG of subjects who are later confirmed to have ischemia due to one or more significant blocks (> 70 %) in coronary arteries based on invasive angiogram alone are considered for the ML classification problem. Institutional human ethics committee constituted by JIPMER, Puducherry, India had granted approval (JIP/IEC/2016/29/963 dated 08.09.2016) for this study. Informed consents are obtained from all the participants of this study.

ECG data of healthy and MI subjects collected from PTB MI database [25], healthy controls ($n = 50$) and subjects with MI ($n = 50$) and another ECG data of subjects with MI ($n = 62$) and healthy controls ($n = 23$) from European ST-T database [26] are used to independently test the efficacy of inter-beat features proposed in this study.

2.3. MCG pre-processing

The raw MCG time series of all the SQUID channels showed cardiac features with SNR varying between 9–28 dB across the measurement channels (15 ± 8 dB, mean $\pm$ standard deviation). The SNR is computed by measuring the peak-to-peak magnitudes of prominent R wave in every MCG channel and the portion of time segment before the onset of P wave (where no cardiac activity is present). An epoch-based de-noising scheme discussed in an earlier work [20] is used to remove low-and-high-frequency artefacts to facilitate beat-by-beat computation of MCG parameters. The method involves segmenting the whole time series in every channel into ensemble of several beats (epochs); each containing a full cardiac cycle aligned with reference to R wave. The time registries of cardiac features across the epochs are then utilized to select common fiducial points before P wave and after T wave by using spline interpolation technique to estimate and subtract drift from each epoch. The baseline-corrected epochs are automatically categorized in to beat groups based on correlation measure. Each beat group is individually subjected to principal component analysis (PCA) to remove uncorrelated high-frequency (HF) noise. The PCA-corrected beats are then restored to their original beat numbers in the cardiac time series. By this way, the de-noising is achieved without affecting the beat-by-beat information of the cardiac beats.

Figure 2 illustrates the pre-processing of MCG time series measured from a subject with IHD showing apparent beat-by-beat variations in ST-T region, but corrupted by low-and- high-frequency noisy variations. The green trace in figure 2 is the raw MCG time series and the baseline-corrected epochs are shown as red traces and the same with HF noise eliminated by PCA are shown as black traces (superposed over red traces). It could be seen that the de-noised beats (black traces) exhibit conspicuous variations in ST segment and the T wave which are essential to be utilized for this study. A significant improvement in SNR (~ 15–25 dB) is achieved by this epoch-based de-noising method [20]. The procedure is also applied on ECG time series to improve the quality of the cardiac time series for easy extraction of features.

2.3.1. Cardiac features of importance for ML classification

2.3.1.1. Choosing cardiac features for this study

A variety of features have been used by researchers in IHD detection, and they basically probe the temporal and spatial heterogeneity of ventricular repolarization that are expected in ischemia [3]. This includes QT dispersion, spatio-temporal parameters of MCG in terms of magnetic field map (MFM) orientation angles, viz., field map angle (FMA) and current angle (CA) and the proportion of de-and-repolarization, magnitude of ST segment etc, These features are widely reported to be used for ML classification in the literature [5, 11, 13, 14]. In addition, two inter-beat measures namely the beat-by-beat alpha angle and the T wave magnitude variations proposed by Hasan and co-workers [22] are also included in this work. Hence, the following set of eight features are computed from a cardiac beat of MCG measurement channels.

2.3.1.2. Measurement of features

Figure 3 shows an overlay plot of de-noised MCG beat of a cardiac cycle measured across 37 channels and the following points describe the computation of each of the feature employed in this work:

(1) R_{max}/T_{max}: Measurement of the tallest R and T waves across MCG channels as indicated in figure 3(a).

(2) QT dispersion (ΔQT): Measurement of the difference between the shortest and the longest QT values in the thirty-seven traces of MCG waveforms as illustrated in figure 3(b).

(3) ST Elevation (ST$\uparrow$) and depression (ST$\downarrow$): The portion of the cardiac cycle after the QRS-offset within a time interval $\sim$ 60–80 ms is taken as the ST segment in this study and any vertically upward or downward variation in its magnitude is respectively taken as ST elevation and ST depression about the time segment before P wave which is taken as the baseline reference.

(4) Magnetic field map-based features at T wave peak: MFM is a spatio-temporal visualization generated by joining roughly equal values of magnetic field values across measurement locations on the chest at any instant of time on the cardiac cycle [23]. The filed map used here is the one generated at the

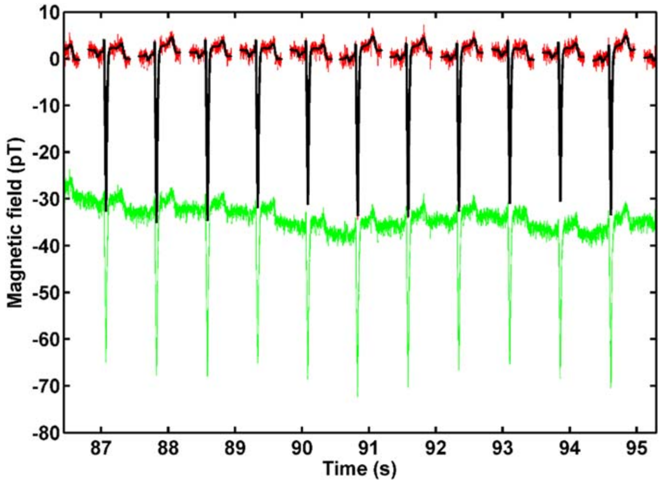

Figure 2. De-noising of MCG time series using epoch-based method. Raw MCG (green trace), Baseline-corrected epochs (red trace), epochs with high-frequency noise eliminated (black traces).

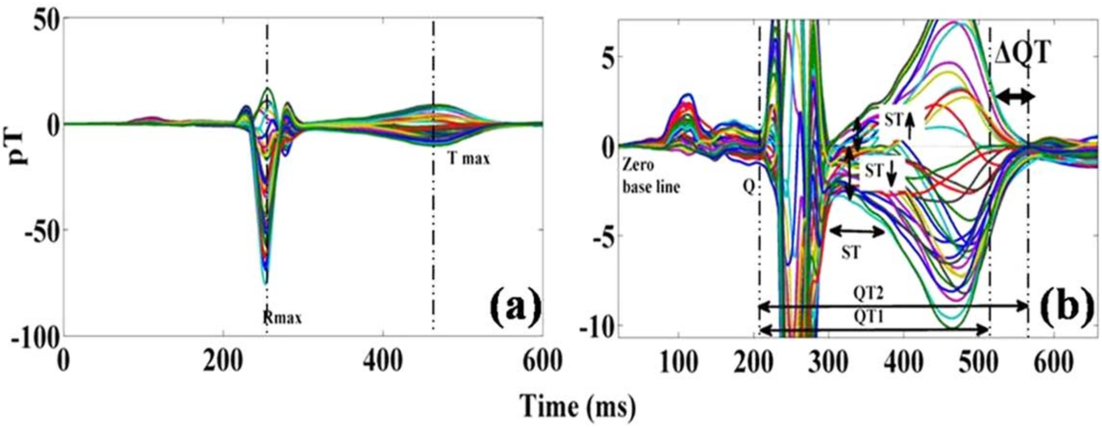

Figure 3. Measurement of features from de-noised cardiac beats for ML classification (a) Overlay plot of a cardiac beat of MCG in thirty-seven measurement locations on the chest. Maximum amplitude values of R and T waves are indicated to measure the feature R_{max}/T_{max} (b) Magnified view of the plot in (a) showing the extraction of maximum and minimum shift in the ST segment and the measurement of the difference in QT intervals.

T wave peak time instant and is shown in figure 4 with the orientation angles viz., CA and FMA that define the field distribution pattern. Taking a spatial derivative on the field distribution pattern gives pseudo current vectors which signify the current dipole vectors [8]. The dipole vector with maximum current density represents the actual current source and the angle subtended by the chosen current vector with the central-line of the sensor array represents the CA. Similarly, the angle subtended by the line-joining the negative and a positive maximum value of the field map with the central-line is FMA [10] as indicated in figure 4.

(5) Beat-by-beat variations in alpha angle ($\Delta\alpha$ angle): A set of fiducial points viz., the QRS-onset, T wave peak, and T wave offset are identified in a chosen measurement channel using an open-source ECGdeli software toolbox [27]. The individual epochs of the de-noised ECG/MCG cardiac time series are subjected one-by-one for the subsequent computation of alpha (α) angle. Figure 5 illustrates alpha angle measurement from the beat epoch of a channel. Calculation of α angle requires formation of a triangle by measuring the Euclidian distances of QRS-onset, T wave peak, and T wave offset in every cardiac beat [22]. In order to calculate the Euclidean distances in forming the vertices of the triangle, every cardiac beat (in figure 5(a)) is represented in a magnitude and time normalized modified scale to have equal weights on the X and Y-axis as shown in figure 5(b). The time axis is re-referenced based on the instant of R wave and the magnitude axis to their maximum values. As shown in figure 5(c), the angle subtended by the vertices of the triangle between the QRS-onset and T wave peak and that of the T wave offset is the alpha angle and could be

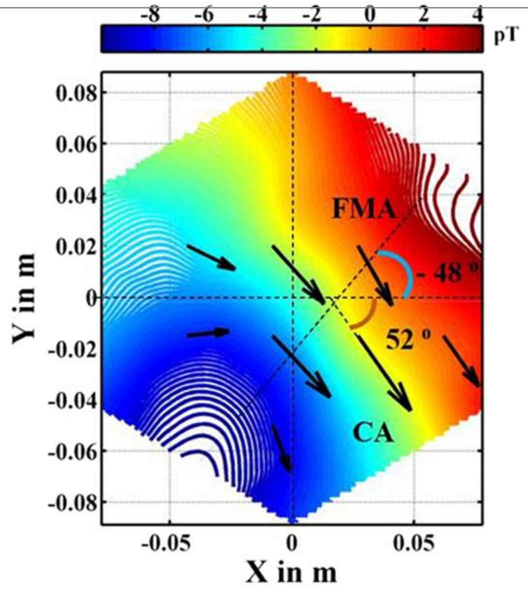

Figure 4. Measurement of MFM-based features at T wave peak instant. Pseudo current density vectors, current (CA) and field map angles (FMA) are also indicated.

calculated by law of cosines following a method described in earlier works [22, 28]. The alpha angle measured in every beat is compared against that measured for the consecutive beat and their absolute values of differences are stored in a beat-by-beat manner. The overall difference in α shown in figure 5(c) is then expressed as a deviation from its mean value expressed in percentage.

(6) Beat-by-beat variations in T wave magnitude (ΔT): Beat-by-beat variations in the magnitude of T wave are also expressed as a percentage variation like alpha angle.

Since computation of spatial orientation features such as FMA and CA from voltage distribution maps in ECG necessitates multiple measurements over the chest, only six features could be used in the case of the two public ECG data sets for MI versus controls.

2.3.2. Machine learning (ML) classifiers

Eight machine learning models are chosen in this study, namely, logistic regression (LR), Naïve Bayesian, K-nearest neighbor (KNN), gradient boosted decision tree (GBDT), support vector machine (SVM), random forest (RF), extended gradient boost (XG Boost), and Adaptive boosting (Ada Boost) classifiers. Choice of this set of classifiers is to have a combination of classical models and advanced algorithms to meet the primary requirements of better accuracies and the suitability of classifiers for a limited and an imbalanced dataset [29]. All the eight classifiers are used in 'k' fold cross validation approach, where in the whole data set is split in to 'k' folds and the training and testing are repeated and the overall performance of the classifier is obtained as the average of each fold. 'k' is fixed as 6 in this study. Scikit-learn library of Python open-source software 3.9.10 (Python software Foundation, Delaware, USA) [30] is used for the classification problem. Table 1 lists hyper parameters of some of these classifiers used in this work chosen based on the suggestions in literature to get the best possible classification [29]. Standard evaluation measures of classifiers viz., Sensitivity (Se), Specificity (Sp), Positive predictive value (PPV), Negative predictive value (NPV), Accuracy (Acc) and F1-Score (F1) are computed for each classifier and are compared.

Table 1. List of hyper parameters for ML classifiers.

Sl. No.	ML classifier	Important hyper parameters
1.	KNN	No. of Neighbors = 5
2.	GBDT	Learning rate = 0.06
3.	Random Forest	No. of estimators = 100, Random state = 42
4.	XG Boost	Random state = 42
5.	Ada Boost	Maximum depth = 1, No. of estimators = 50, Random state = 42

3. Results

3.1. ML classification of IHD and control subjects in MCG

Table 2 presents the classifier outputs of the first four best outcomes obtained in this work. The two columns of each classifier shown in the Table represent the outcomes pertaining to the conventional choice of features (without beat-by-beat features) and an optimal choice of features (viz., ΔT, $\Delta\alpha$, and FMA). This optimal choice of features is chosen based on higher values of area under the receiver operating characteristic curve (AUROC) (> = 0.70) when all the eight features

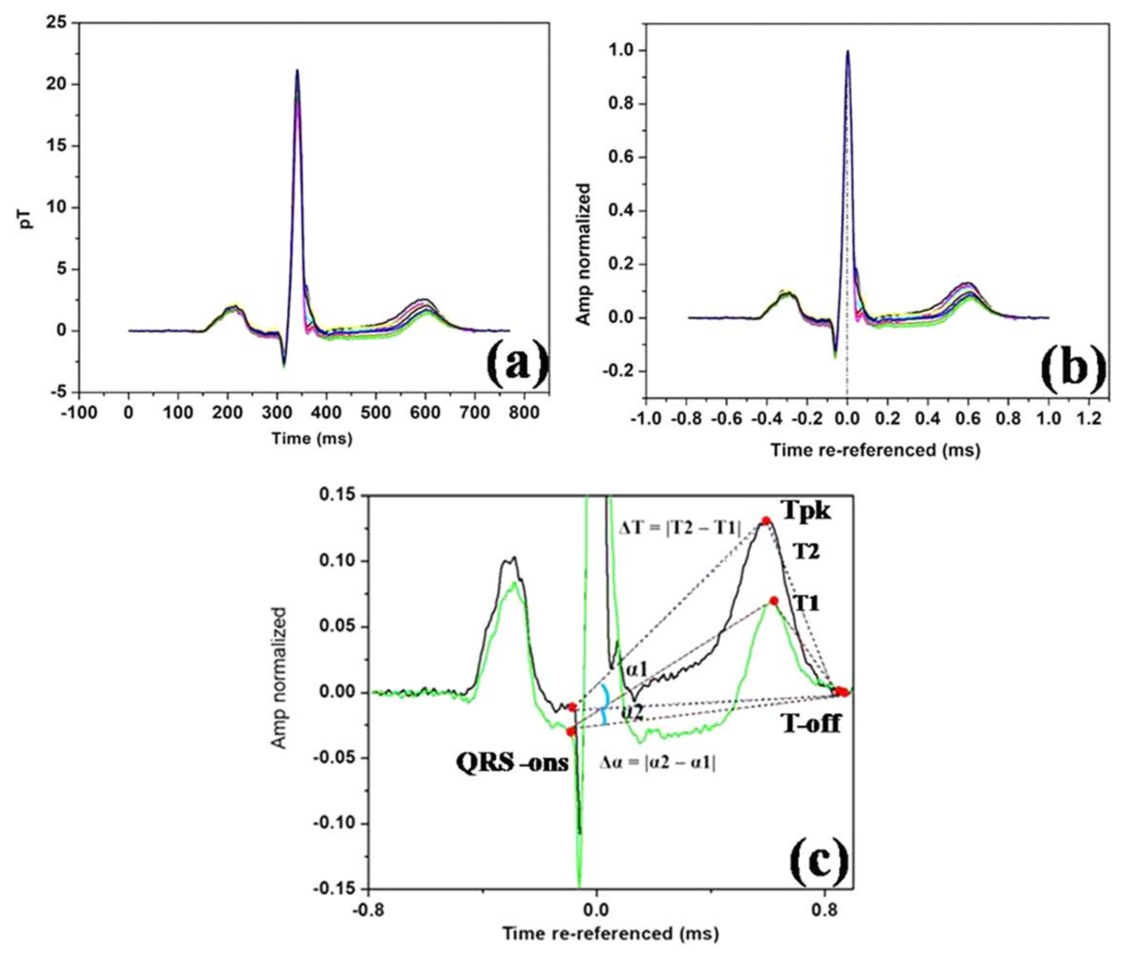

Figure 5. Measurement of beat-by-beat features from MCG time series (a) De-noised cardiac epochs (b) Time scale of the epochs re-referenced to R peak instants and amplitude values normalized about maximum values (c) Formation of triangle by joining the fiducial points, QRS-onset, T peak and T offset and calculation of alpha angle and T wave variations in two representative beats by law of cosines.

Table 2. Comparison of performance of ML classifiers for the conventional and optimal choice of features in MCG.

	SVM		XG Boost		Ada Boost		RF	
	CA, FMA, ST↑, ΔQT, R/T	ΔT, Δα, FMA	CA, FMA, ST↑, ΔQT, R/T	ΔT, Δα, FMA	CA, FMA, ST↑, ΔQT, R/T	ΔT, Δα, FMA	CA, FMA, ST↑, ΔQT, R/T	ΔT, Δα, FMA
Se (%)	56	71.4	55	81	50	80	63	82.6
Sp (%)	85	90.7	87	93.4	85	92.2	85	95.9
PPV (%)	45	68.2	55	77.2	50	72.7	65	86.3
NPV (%)	89	92	87	94.6	85	94.6	92	94.6
Acc (%)	79	86.6	77	90.7	77	89.6	81	92.7
F1 (%)	50	69.7	50	79.1	50	76.2	63	84.4

are tested for their individual performance as given in the supplementary information. As shown in table 2, since the conventional choice of features (without beat-by-beat features) could be computed even from signal-averaged MCG waveforms if employed could deliver only inferior performance (92.7 versus 81 %). Random forest classifier achieves the best outcomes among the four classifiers. Figure 6 depicts the variations in performances of RF classifier for different combinations of the feature sets and the best outcome corresponds to the set of features, ΔT, Δα, and FMA. It is also to be noticed that the two beat-by-beat features i.e., ΔT, Δα alone could not achieve the best performance and only their combination with the conventional MCG-MFM feature, namely the FMA gives the best outcome. RF could correctly classify 19 out of 23 IHD subjects (True positive) and 3 are misclassified (i.e., False positive). Similarly, the classifier could correctly identify 71 out of 75 healthy controls (i.e., True negative) and 4 are misclassified (i.e., False negative).

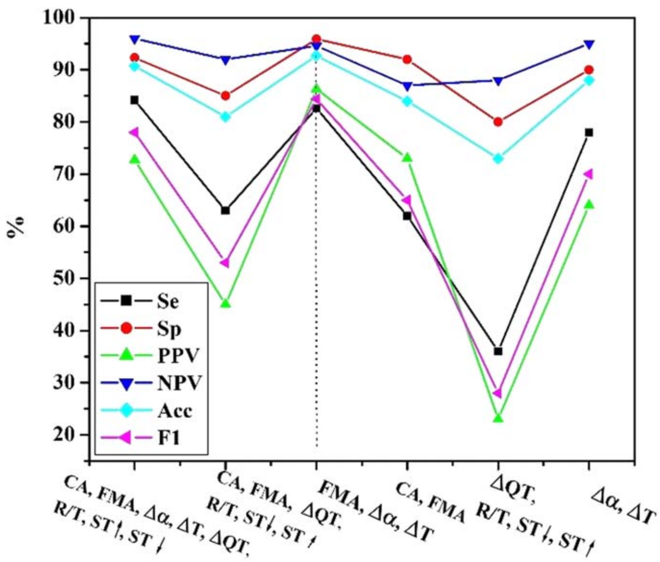

Figure 6. Performance of RF classifier for classifying IHD and healthy controls for varying combinations of MCG feature sets.

3.2. ML classification of MI in ECG

Tables 3 and 4 list the performances of four best classifiers in classifying MI against controls in the two public ECG databases. Like table 2, the conventional and an optimal choices of feature sets are guided by the AUROC curves of respective cases as given in the supplementary information. XG Boost and Ada Boost are found to outperform other classifiers respectively in the two ECG-MI datasets and like MCG, the optimal choice which include the beat-by-beat features alone could achieve the best outcomes (92 % Versus 88 in PTB-MI and 94 % Versus 77 % in European ST-T). It is clear from all these cases, the beat-by-beat features augment classification accuracy.

For the PTB-MI database, XG Boost could correctly classify 45 out of 50 (MI subjects) and 5 are misclassified (i.e., False positive), 47 healthy controls could be correctly identified (True negative) and 3 are misclassified (False negative). Similarly, in European ST-T database, Ada Boost classifier could correctly identify 23 out of 24 MI subjects (True positive) and 1 is misclassified (False positive). Twenty-two out of 24 are correctly identified as healthy (True negative) and two are misclassified (False negative). Figure 7 shows the variations in performances of the respective best classifiers applied on the data from the two ECG databases (figures 7(a) and (b) respectively). In accordance with the results obtained in MCG, the optimal choice of the feature set inclusive of beat-by-beat and some conventional features only could offer the best classifier outcomes in MI Versus controls.

4. Discussion

4.1. MCG results

Extraction of relevant features in ST-T region using highly sensitive modality like MCG signals is posed with a challenge of not missing subtle variations associated with ischemia (where the modality has an inherent sensitivity to record them) and further in choosing a correct set of features that aids in objective classification of healthy and IHD subjects. The present work has attempted to accomplish this task with a set of conventional and inter-beat features. Table 5 compares the ML classification achieved in the present study against some of the reported works on ML detection of IHD in MCG.

The following observations are made from table 5:

(a) The classification accuracy of the present work is better than that achieved in most of the earlier works except a few reports [12, 16]. However, the accuracy of the present work is comparable with a study performed with the highest number of features (164 features, the highest number used so far in this subject area of research in MCG) [16], i.e., 92.7 % versus 94.03%.

(b) The sensitivity that could be obtained in this work (82.6 %) requires further improvement as compared to most of the earlier works, but the obtained specificity (95.9 %) is higher than the other reports except that found in the work of Steinisch and co-workers [12] that has achieved the best classifier outcomes in ML identification of IHD using MCG and the only study which has used inter-beat features in MCG to our knowledge. However, it is to be noted that the number of cases considered for classification by Steinisch and co-workers [12] is small (4 IHD and 6 controls), and hence, the comparison of the present results on MCG may not be straightforward. Nevertheless, that work had classified individual beats of normal and ischemic subjects to improve the sample size and is worth investigating for a comprehensive assessment. Hence, it

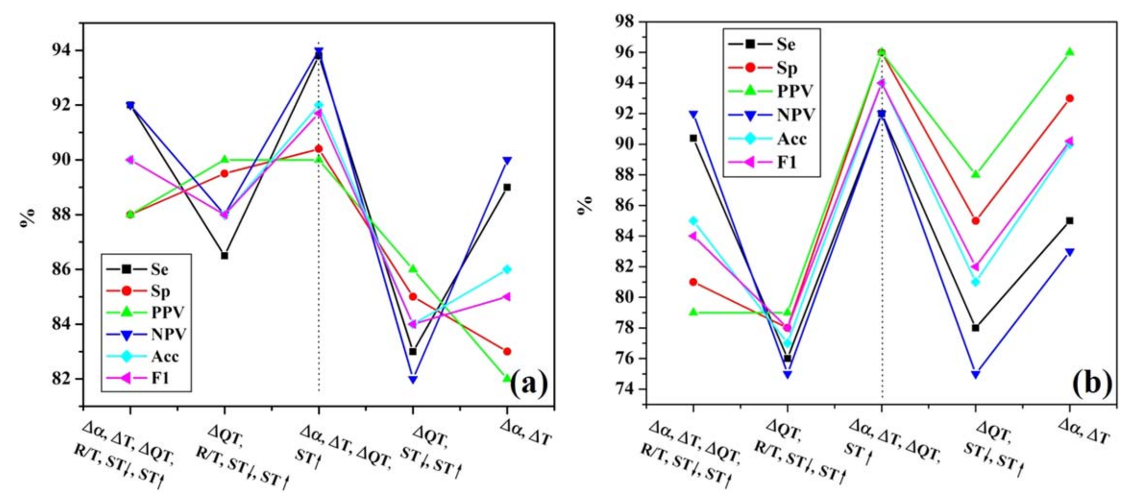

Figure 7. Performance of XG Boost and Ada Boost classifiers for classifying MI and healthy controls for different combinations of features in ECG datasets (a) PTB-MI (b) European ST-T.

Table 3. Comparison of performance of ML classifiers for the conventional and optimal choice of features in PTB-MI ECG.

	LR		RF		XG Boost		GBDT	
	ΔQT, ST↑, R/T	Δα, ΔQT, ΔT, ST↑	ΔQT, ST↑, R/T	Δα, ΔQT, ΔT, ST↑	ΔQT, ST↑, R/T	Δα, ΔQT, ΔT, ST↑	ΔQT, ST↑, R/T	Δα, ΔQT, ΔT, ST↑
Se (%)	74	82	88	91	86.5	93.8	75	90.2
Sp (%)	92	89	44	88	89.5	90.4	76	90
PPV (%)	94	90.2	88	86	90	90	76	90.2
NPV (%)	66	80	44	92	88	94	74	90
Acc (%)	80	85.1	80	89	88	92	75	90
F1 (%)	83	86	88	89	88	91.7	76	90.2

Table 4. Comparison of performance of ML classifiers for the conventional and optimal choice of features in European ST-T ECG.

	Bayesian		XG Boost		RF		Ada Boost	
	ΔQT, ST↑, ST↓, R/T	ΔQT, ST↑, ΔT, Δα	ΔQT, ST↑, ST↓, R/T	ΔQT, ST↑, ΔT, Δα	ΔQT, ST↑, ST↓, R/T	ΔQT, ST↑, ΔT, Δα	ΔQT, ST↑, ST↓, R/T	ΔQT, ST↑, ΔT, Δα
Se (%)	71	91	68	86	72	85	76	92
Sp (%)	88	88	75	78	74	92.2	78	96
PPV (%)	92	88	79	75	75	92	79	96
NPV (%)	63	92	63	88	71	83	75	92
Acc (%)	77	90	71	81	73	88	77	94
F1 (%)	80	89	73	80	73	88	78	94

stands as one of the limitations of the present work. Secondly, apart from spatial and temporal features, indices based on entropy measures have not been considered in this work. It is possible that inclusion of such information theory-based features and its beat-by-beat computation might further improve the classifier outcomes.

4.2. Results from ECG databases

Tables 6 and 7 present the comparison of the performance of some of the recent works which have used the same two ECG public databases in classifying MI and healthy controls. All the reported works in the Tables have used individual cardiac beats and inter-lead ECG features in some sense similar to the inter-beat features used in the present work. It could be seen that the classifiers used in the present work with chosen feature sets are comparable with the performance of all these reported works and have achieved reasonable outcomes with a only a few, but optimal selection of conventional and inter-beat features that are derived directly from any clean ECG/MCG time series.

Hence, as a general observation, an internal consistency could be seen in the performance of the beat-by-beat features in identifying ischemia in MCG and ECG. These results summarily highlight the

Table 5. Comparison of the results of ML detection of IHD using MCG.

Sl. no	Reported works	Features	Classification approach	Se %	Sp %	Acc %
1.	Steinisch *et al* (2013) [12]	Signal entropy of QRS and ST-T in every beat	Multi-Layer Perceptron (MLP)	99	98	98
2.	Chaikovsky *et al* (2017) [15]	32 features inclusive of geometric measures from current arrow maps	KNN	93	89	91
3.	Tao *et al* (2019) [16]	164 features (time domain, frequency domain, information theory-based parameters)	XG Boost	97.7	—	94.03
4.	Huang *et al* (2020) [17]	10 features derived from MFM	MLP—Model 1	89.8	88.9	89.5
			MLP—Model 2	91.4	87.7	90.0
5.	Hu *et al* (2022) [19]	Current arrow map-based features	Deep learning-Residual network	—	—	90.02
6.	Tao *et al* (2022) [18]	Automated delineation and extraction of MFM-based features	Convolutional neural network and Transformer encoder in Deep learning architecture	73.2	91.4	87
7.	Present study	FMA, $\Delta\alpha$, ΔT	Random Forest classifier	82.6	95.9	92.7

Table 6. Comparison of results on ML classification on PTB-MI database.

Sl. no	Reported works	Features	ML classifier	Se %	Sp %	Acc %
1.	Yang *et al* (2022) [31]	Beat to sub waves bands ± cascaded CNN to extract features	LR	92	88	91
			SVM	92	81	90
2.	Chauhan *et al* (2023) [32]	Formation of 3D Tensor from beats, leads and samples	KNN	96.1	98.5	97.9
3.	Present study	ΔQT, ΔT, ST$\uparrow$, $\Delta\alpha$	XG Boost	93.8	90.4	92.1

Table 7. Comparison of results on ML classification on European ST-T database.

	Reported works	Features	ML classifier	Se %	Sp %	Acc %
1.	Tseng *et al* (2016) [33]	ΔST, ST slope, T magnitude, ST area, J80 amplitude, T/R ratio	Sparse representation convolution	96	96	—
2.	Kayikcioglu *et al* (2020) [34]	Time and frequency distribution-based features from multi lead ECG	Weighted- kNN	95.7	98.1	94.3
3.	Present study	ΔQT, ΔT, $\Delta\alpha$, R/T	Ada Boost	92	96	94

involvement of beat-by-beat features in augmenting the detection capability of early (IHD) to a matured state (MI) of ischemic conditions. However, there is a lot of scope to further improve the diagnostic outcomes. MCG being a safe, sensitive and a noninvasive modality, ML detection of ischemia under rest condition underscores its clinical application in effectively prioritizing subjects for an efficient clinical management.

5. Conclusion

The use of beat-by-beat cardiac features in ML classification of ischemia and MI has been demonstrated using MCG and ECG of subjects. Since the signal variations of IHD are weaker than the more pronounced manifestations of MI, the sensitivity of MCG in measuring these variations are observed to be effectively probed by the chosen set of features and their individual and combined roles are evaluated. These results are important since IHD are ahead in the time evolution of MI and ML models would offer better diagnostic outcomes if equipped with features which contain early signatures of ischemia in the ST-T region.

Acknowledgments

The authors thank all those who had helped to compile this work as a manuscript. The authors also thank anonymous reviewers whose comments have helped to enrich the technical content. The author SS thanks Dr Pathan Fayaz Khan, and Mr C Kesavaraja for useful discussions on ML classifiers.

Data availability statement

No new data were created or analysed in this study.

Conflict of interest

There are no conflicts of interest for any of the author of this manuscript. No specific funding has been obtained from the institutions of the authors to carry out this research work.

Ethics statement

Institutional human ethics committee of JIPMER, Pondicherry had approved the research reported in this work (JIP/IEC/2016/29/963 dated 08.09.2016). All subjects gave informed consent.

ORCID iDs

S Senthilnathan https://orcid.org/0000-0002-4444-7918

References

[1] Kumar A S and Sinha N 2020 Cardiovascular disease in India: a 360 degree overview *Med. J. Arm. Fr. Ind.* **76** 1–3

[2] Khan M A B *et al* 2020 Global epidemiology of ischemic heart disease: results from the global burden of disease study *Cureus* **12** e9349

[3] Sirajuddin A, Mirmomen A M, Kligerman S J, Groves D W, Burke A P, Kureshi F, White C S and Arai A E 2021 Ischemic heart disease: noninvasive imaging techniques and findings *RadioGraphics* **41** 990–1021

[4] Her A Y, Dischl D, Kim Y H, Kim S W and Shin E S 2023 Magnetocardiography for the detection of myocardial ischemia *Front Cardiovasc Med.* **10** 1242215

[5] Ramesh R, Senthilnathan S, Satheesh S, Patel R, Swain P P, Gireesan K and Raja J S 2020 Magnetocardiography for identification of coronary ischemia in patients with chest pain and normal resting 12-lead electrocardiogram *Ann Noninv Electrocardiol* **25** e12715

[6] Smith F E, Langley P, Leeuwen P V, Hailer B, Trahms L, Steinhoff U, Bourke J P and Murray A 2007 Comparison of magnetocardiography and electrocardiography *Anatol J. of Cardiol* **7** 20–2

[7] Fenici R and Brisinda D 2007 Predictive value of rest magnetocardiography in patients with stable angina *Int. Cong. Series* **1300** 737–40
[8] Yamada S and Yamaguchi I 2005 Magnetocardiograms in Clinical medicine: unique information on cardiac ischemia, arrhythmias, and fetal diagnosis *Int. Med.* **44** 1–19
[9] Pena M E, Pearson C L, Goulet M P, Kazan V M, DeRita A L, Szpunar S M and Dunne R B 2020 A 90-second magnetocardiogram using a novel analysis system to assess for coronary artery stenosis in emergency department observation unit chest pain patients *Int. J. of Cardiol: Hrt. & Vascul* **26** 100466
[10] Lim H K, Chung N, Ko Y G, Lee Y H and Park Y K 2009 Magnetocardiogram difference between healthy subjects and ischemic heart disease patients *IEEE Trans. Mag.* **45** 2890–3
[11] Kangwanariyakul Y, Nantasenamat C, Tantimongcolwat T and Naenna T 2010 Data mining of magnetocardiograms for prediction of ischemic heart disease *EXCLI J.* **9** 82–95
[12] Steinisch M, Torke P R, Haueisen J, Hailer B, Gronemeyer D, Leeuwen P V and Comani S 2013 Early detection of coronary artery disease in pateints studied with magnetocardiography: an automatic classification system based on signal entropy *Comp. Biol. & Med.* **43** 144–53
[13] Wu Y W, Lin L C, Tseng W K, Liu Y B, Kao H L, Lin M S and Wu C C 2014 QTc heterogeneity in rest magnetocardiography is sensitive to detect coronary artery disease in comparison with stress perfusion imaging *Acta Cardiolog. Sca.* **30** 445–54
[14] Li Y, Che Z, Quan W, Yuan R, Shen Y, Liu Z, Wang W, Jin H and Lu G 2015 Diagnostic outcomes of magnetocardiography in patients with coronary artery disease *Int. J. of Clin. and Exp. Med.* **8** 2441–6
[15] Chaikovsky I *et al* 2017 Coronary artery disease versus coronary microvascular disease: advanced analysis of magnetocardiographic maps *J. of Am Coll. Cardiol* 70 (16_Supplement)C88
[16] Tao R *et al* 2019 Magnetocardiography-based Ischemic Heart disease detection and localization using machine learning methods *IEEE Trans. BioMed Engg.* **66** 1658–67
[17] Huang X, Chen P, Tang F and Hua N 2020 Detection of coronary artery disease in pateints with chest pain: a machine learning model based on magnetocardiography parameters *Clin. Hemorheol. Microcirc.* **78** 1–10
[18] Tao R, Zhang S, Wang Y, Mi X, Ma J, Ma S and Zheng G 2022 MCG-net: end-to-end fine-grainded delineation and diagnostic classificiation of cardiac events from Magnetocardiographs *IEEE J. Biomed. & Health Inform* **26** 10571067
[19] Hu Z, Lin Y, Ye K and Lin Q 2022 Classification of current density vector maps for heart failures using a transfer convolutional neural network *IEEE Access* **10** 82766–75
[20] Sengottuvel S, Shenbaga Devi S, Sasikala M, Satheesh S and Selvaraj R J 2021 An epoch based methodology to denoise magnetocardiogram (MCG) signals and its application to measurements on subjects with implanted devices *Biomed. Phys. Eng. Express* **7** 1–14
[21] Mollo R *et al* 2012 T-wave alternans in apparently healthy subjects and in different subsets of patients with ischaemic heart disease *EP Europace* **14** 272–7
[22] Hasan M A, Abbott D, Baumert M and Krishnan S 2018 Increased beat-to-beat T-wave variability in myocardial infarction patients *Biomed. Eng. Technik.* **63** 123–30
[23] Janawadkar M P, Radhakrishnan T S, Gireesan K, Parasakthi C, Sengottuvel S, Patel R, Sundar C S and Raj B 2010 SQUID-based measurement of biomagnetic fields *Curr. Sci.* **99** 36–45
[24] Parasakthi C, Patel R, Sengottuvel S, Mariyappa N, Gireesan K, Janawadkar M P and Radhakrishnan T S 2012 Establishment of 37 channel SQUID system for magnetocardiography *AIP Conf. Proc.* **1447** 871–2
[25] Bousseljot R, Kreiseler D, Schnabel A and Nutzung der 1995 EKG-Signal datenbank CARDIODAT det PTB uber das Internet *Biomedizinesche Technik Band* **40** Erganzungsband 1 S 317
[26] Taddei A, Distante G, Emdin M, Pisani P, Moody G B, Zeelenberg C and Marchesi C 1992 The European ST-T database: standard for evaluating systems for the analysis of ST-T changes in ambulatory electrocardiography *Eur. Hr. J.* **13** 1164–72
[27] Pilia N, Nagel C, Lenis G, Becker S, Dossel O and Loewe A 2020 ECGdeli- an open-source ECG delineation toolbox for MATLAB *SoftwareX* **13** 100639
[28] Brummelen G V 2012 *In Book, Heavenly Mathematics: The Forgotten Art of Spherical Trignometery* (Princeton University Press) Ch. 6
[29] Mulugeta G, Zewotir T, Tegegne A S, Juhar L H and Muleta M B 2023 Classification of imbalanced data using ML algorithms to predict the risk of renal graft failures in Ethiopia *BMC Med Inform and Decis Mak* **23** 98
[30] Muller A C and Guido S 2016 *Introduction to machine learning with python* (O'reilly Media Inc)
[31] Yang Y, Rocher M, Moceri P and Sermesant M 2022 *Explainable Electrocardiogram Analysis with Wave Decomposition: Application to Myocardial Infarction Detection STACOM 2022-13th workshop on Statistical Atlases and Computational Models of the Heart (Singapore, September, 2022)* Inra HAL Preprint Server, HAL id: hal-03888791
[32] Chauhan C, Tripathy R K and Agarwal M 2023 Tensor-domain ML based cardiac disease detection using 12-Lead ECG *Proc. National Conf on Comm (NCC-2023)* 1–5
[33] Tseng Y L, Lin K S and Jaw F S 2016 Comparison of support vector machine and sparse representation using a modified rule-based method for automated myocardial ischemia detection *Comp. & Math. Meth. Med.* **2016** 1–8
[34] Kayikcioglu I, Akdeniz F, Kose C and Kayikcioglu T 2020 Time-frequency approach to ECG classification of myocardial infarction *Comp. & Elect. Engg.* **84** 106621